Distinctive localization and opposed roles of vasohibin-1 and vasohibin-2 in the regulation of angiogenesis

Hiroshi Kimura,[1,2] Hiroki Miyashita,[1] Yasuhiro Suzuki,[1] Miho Kobayashi,[1] Kazuhide Watanabe,[1] Hikaru Sonoda,[3] Hideki Ohta,[3] Takashi Fujiwara,[4] Tooru Shimosegawa,[2] and Yasufumi Sato[1]

[1]Department of Vascular Biology, Institute of Development, Aging, and Cancer, Tohoku University, Sendai; [2]Department of Gastroenterology, Tohoku University Graduate School of Medicine, Sendai; [3]Discovery Research Laboratories, Shionogi and Co, Osaka; and [4]Department of Biological Resources, Integrated Center for Science (INCS), Ehime University, Shitsukawa, Ehime, Japan

We recently isolated a novel angiogenesis inhibitor, vasohibin-1, and its homologue, vasohibin-2. In this study we characterize the role of these 2 molecules in the regulation of angiogenesis. In a mouse model of subcutaneous angiogenesis, the expression of endogenous vasohibin-1 was low in proliferating ECs at the sprouting front but high in nonproliferating endothelial cells (ECs) in the termination zone. In contrast, endogenous vasohibin-2 was preferentially expressed in mononuclear cells mobilized from bone marrow that infiltrated the sprouting front. When applied exogenously, vasohibin-1 inhibited angiogenesis at the sprouting front where endogenous vasohibin-1 was scarce but did not influence vascularity in the termination zone where endogenous vasohibin-1 was enriched. Exogenous vasohibin-2 prevented the termination of angiogenesis in the termination zone and increased vascularity in this region. Angiogenesis was persistent in the termination zone in the *vasohibin-1* knockout mice, whereas angiogenesis was deficient at the sprouting front in the *vasohibin-2* knockout mice. Supplementation of deficient proteins normalized the abnormal patterns of angiogenesis in the vasohibin knockout mice. These results indicate that vasohibin-1 is expressed in ECs in the termination zone to halt angiogenesis, whereas vasohibin-2 is expressed in infiltrating mononuclear cells in the sprouting front to promote angiogenesis. (Blood. 2009; 113:4810-4818)

Introduction

Angiogenesis, or the formation of new capillaries, is a key event in various developmental or remodeling processes that take place under physiologic and pathologic conditions. Angiogenesis is a dynamic phenomenon that involves sequential processes. The initial event is the detachment of mural pericytes from preexisting vessels for vascular destabilization. Subsequently, specialized endothelial cells (ECs) at the tip of sprout, called tip cells, degrade the basement membrane and extracellular matrices and actively migrate. The stalk cells follow the tip cells, proliferate, and form tubes. Finally, pericytes reattach to the new vessels as they mature. Through these processes, a new hierarchical vascular architecture will be constructed.[1]

The local balance between angiogenesis stimulators and inhibitors determines whether angiogenesis will be switched on. Numerous endogenous angiogenesis inhibitors are found in the body and play distinctive roles.[2] For example, molecules such as pigment epithelium-derived factor,[3,4] chondromodulin-1,[5,6] and maspin[7,8] are localized extrinsic to the vasculature and block the intrusion of new vessels as functional barriers. Thrombospondin-1 and thrombospondin-2 are deployed mainly by platelets and turn the angiogenic switch off.[9] Moreover, several angiogenesis inhibitors, including endostatin and tumstatin, are generated by the degradation of the basement membrane during angiogenesis.[10] Besides them, ECs themselves have the capacity to synthesize certain inhibitors that autoregulate angiogenesis.[2]

By searching for novel and functional vascular endothelial growth factor (VEGF)–inducible molecules in ECs, we isolated one angiogenesis inhibitor and named it vasohibin-1 (VASH1).[11] VASH1 is induced in cultured ECs by representative angiogenic growth factors, such as VEGF and fibroblast growth factor 2 (FGF-2), and is detected selectively in ECs at the site of angiogenesis in vivo.[11] The inducible expression of VASH1 in ECs is impaired by tumor necrosis factor-α, interleukin-1, or hypoxia.[11,12] Human VASH1 protein is composed of 365 amino acid residues. VASH1 lacks a classical secretion signal sequence but is released extracellulary, indicating that VASH1 is an unconventional secretory protein.[11,13] When applied exogenously, VASH1 inhibits the migration and proliferation of ECs stimulated with either VEGF or FGF-2.[11] This inhibitory effect is not due to the inactivation of growth factor signals, because VASH1 does not affect VEGF receptor 2 or ERK1/2 phosphorylation in ECs on VEGF simulation.[11] VASH1 exerts antiangiogenic activity under various pathologic conditions such as those of tumors, retinal neovascularization, and arterial intimal thickening, implying a possible clinical application.[11,14,15]

Through a DNA sequence search of genomic databases, we found one gene homologous to VASH1 and named it vasohibin-2 (VASH2).[16] The genes for human *VASH1* and *VASH2* are located on chromosome 14q24.3 and 1q32.3, respectively.[17] Human vasohibin-2 is composed of 355 amino acid residues, and the overall homology between human VASH1 and VASH2 is 52.5% at

Submitted July 23, 2008; accepted January 27, 2009. Prepublished online as *Blood* First Edition paper, February 9, 2009; DOI 10.1182/blood-2008-07-170316.

The online version of this article contains a data supplement.

The publication costs of this article were defrayed in part by page charge payment. Therefore, and solely to indicate this fact, this article is hereby marked "advertisement" in accordance with 18 USC section 1734.

the amino acid level. Similar to VASH1, any known functional motifs are found in the primary structure of VASH2.

The expression of VASH2 in cultured ECs is very low and is not inducible, but VASH1 and VASH2 proteins are comparably detected in ECs in the developing organs of embryos.[16] We have shown that VASH1 and VASH2 are diffusely expressed in ECs in embryonic organs during mid-gestation. After that time point, they become faint but persisted to a certain extent from late-gestation to neonate. Nevertheless, the function of these 2 molecules remained to be elucidated.

Here, we examined the roles of VASH1 and VASH2 in the regulation of postnatal angiogenesis in detail. For this purpose, we used a simple and reproducible model of postnatal angiogenesis in mice. To our surprise, the spatiotemporal expression patterns of VASH1 and VASH2 were distinct, with VASH1 present in ECs where angiogenesis terminated and with VASH2 present in bone marrow–derived mononuclear cells (MNCs) at the sprouting front. Furthermore, a loss-of-function experiment using knockout mice, as well as a gain-of-function experiment using adenovirus-mediated gene transfer, showed that VASH1 and VASH2 play distinctive roles in the regulation of angiogenesis.

Methods

Mouse model of hypoxia-mediated subcutaneous angiogenesis

All animal studies were reviewed and approved by the committee for animal study in the Institute of Development, Aging, and Cancer at Tohoku University.

A mouse model of subcutaneous angiogenesis was performed in accordance with the method described by Tepper et al.[18] Briefly, after anesthetization, bilateral incisions (2.5 cm in length and 1.25 cm in distance) were made on the dorsal skin of male C57BL/6 mice (Clea, Tokyo, Japan) that penetrated the cutis, dermis, and underlying adipose tissue. A silicon sheet was inserted beneath the flap, and the incisions were closed. In some experiments, adenovirus vector encoding the human *VASH1* gene (AdVASH1),[11] AdVASH2, or adenoviral vector encoding *β-galactosidase* gene (AdLacZ; 10^9 plaque-forming units was injected into the tail vein.[15] AdVASH2 was prepared in accordance with the method described.[11] Seven days after skin surgery, the mice were killed, and the skin flaps were collected for histologic analyses.

For the detection of hypoxic areas, mice were intravenously injected with pimonidazole (Chemicon International, Temecula, CA) 30 minutes before collecting the flap. Hypoxic areas were detected with the Hypoxyprobe-1 mAb1 (Chemicon International).

Generation of *VASH1* and *VASH2* knockout mice

For the construction of the *VASH1* targeting vector, a 7.6-kb genomic fragment upstream of exon 1 and a 2.4-kb genomic fragment downstream of exon 2 were subcloned. The region was designed such that the short homology arm (SA) extends 2.4 kb to 5′ end of loxP/FRT flanked Neo cassette, and the long homology arm (LA) starts at the 3′ side of loxP/FRT flanked Neo cassette. For the construction of the *VASH2* targeting vector, a 7.8-kb genomic fragment upstream of exon 3 and a 2.4-kb genomic fragment downstream of exon 3 were subcloned. The region was designed such that the SA extended 2.4 kb to the 5′ side of the Neo cassette, and the LA started at the 5′ side of LacZ cassette. The loxP/FRT flanked Neo cassette replaced 6.6 kb of the *VASH1* gene, including exon 1 (including the ATG start codon), whereas exon 3 of the *VASH2* gene was replaced with the LacZ/Neo cassette.

Targeted alleles were generated by homologous recombination in embryonic stem (ES) cells of C57BL/6 background. The ES cells carrying each of the targeted alleles were injected into C57BL/6 mouse blastocysts to produce chimeric mice. Chimeras were mated with C57BL/6 females to obtain F1 mice carrying each of the targeted alleles.

Immunohistologic analysis

For immunohistochemical analysis of the skin flap, specimens were frozen in OCT compound (Sakura, Tokyo, Japan), sliced into 10-μm sections, and fixed in methanol for 20 minutes at −20°C. Primary antibody reactions were performed at a dilution of 1:200 for CD31 (rat anti–mouse CD31 mAb; Research Diagnosis, Flanders, NJ), α smooth muscle actin (αSMA) (mouse anti–mouse αSMA mAb; Sigma-Aldrich, St Louis, MO), lymphatic vessel endothelial hyaluronate receptor 1 (LYVE-1; rabbit anti–mouse LYVE-1 polyclonal Ab; Acris Antibodies, Himmelreich, Germany), PCNA (mouse anti–mouse PCNA mAb; Santa Cruz Biotechnology, Santa Cruz, CA), CD11b (goat anti–mouse CD11b polyclonal Ab; Santa Cruz Biotechnology), and macrophage-specific antigen F4/80 (rat anti–mouse F4/80 mAb; Acris Antibodies) and at 1:400 for mouse VASH1 (rabbit anti–mouse VASH1 polyclonal Ab)[16] and VASH2 (rabbit anti–mouse VASH 2 polyclonal Ab)[16] overnight at 4°C. Specificities of anti–mouse VASH1 and anti–mouse VASH2 antibodies have been shown previously.[16] Secondary antibody reactions were performed at a dilution of 1:1500 of the appropriate Alexa 488–, Alexa 568–, or Alexa 594–conjugated donkey secondary Abs (Molecular Probes, Eugene, OR) for 1 hour at room temperature. The vascular luminal area was calculated from 5 different high-power fields.

For whole-mount immunohistochemical analysis of ear skin, the ear skin was prepared according to the method described by Oike et al.[19] Briefly, ear skin was fixed with 4% paraformaldehyde in PBS for 2 hours, permeabilized with methanol, and blocked in 5% sheep serum in 0.3% Triton X-100 (Sigma-Aldrich) in PBS. Primary antibodies and secondary antibodies were incubated overnight at 4°C.

All the samples were analyzed with a Fluoview FV1000 confocal fluorescence microscope (Olympus, Tokyo, Japan) with an UPLSAP 10× or 40× objective lens at room temperature. Fluorochromes used were Alexa 488, Alexa 594, fluorescein isothiocyanate (FITC), or green fluorescent protein (GFP). We used Olympus Fluoview software.

Scanning electron microscopy

Ear skin was obtained and fixed with 3% glutaraldehyde in 0.1 M phosphate buffer (pH 7.4). The method of scanning electron microscopy (SEM) observation was as previously reported.[20] In brief, the specimens were treated with 1% to 2% sodium hypochlorite solution for 45 to 100 seconds, hydrolyzed with 8N HCl for 30 minutes, postfixed with 1% OsO_4, treated with 1% tannic acid solution, and again with 1% OsO_4. After a brief rinse, the specimens were dehydrated through a graded series of ethanol, immersed in t-butyl alcohol, freeze-dried, coated with platinum, and observed with an SEM (Hitachi S-800; Hitachi, Tokyo, Japan).

Detection of vessel perfusion

For the detection of blood vessels with perfusion, mice were infused with FITC-labeled concanavalin A (Sigma-Aldrich) by intracardiac injection before the collection of skin flap. Thereafter, samples were analyzed using a confocal fluorescence microscope (Olympus).

Bone marrow transplantation

Wild-type mice were lethally irradiated with 1 dose of 9 Gy. Thereafter, bone marrow cells harvested from GFP-mice (generous gift from Dr Okabe, Osaka University, Osaka, Japan) that had been purified by density centrifugation (Ficoll-paque PLUS; Amersham Biosciences, Uppsala, Sweden), were transplanted into the wild-type mice (5×10^6 cells/animal). All the recipient mice were given a minimum of 6 weeks of rest to allow for complete bone marrow reconstitution. The engraftment efficiency was determined by fluorescence-activated cell sorting (FACS; FACS Vantage; Becton Dickinson, San Jose, CA) for GFP expression in the bone marrow of mice receiving transplants of GFP-positive bone marrow cells.

Cells

Human umbilical vein endothelial cells (HUVECs) were obtained from KURABO Industries (Osaka, Japan) and were cultured on type-1 collagen–coated dishes (IWAKI, Chiba, Japan) in 10% fetal bovine serum (FBS)/

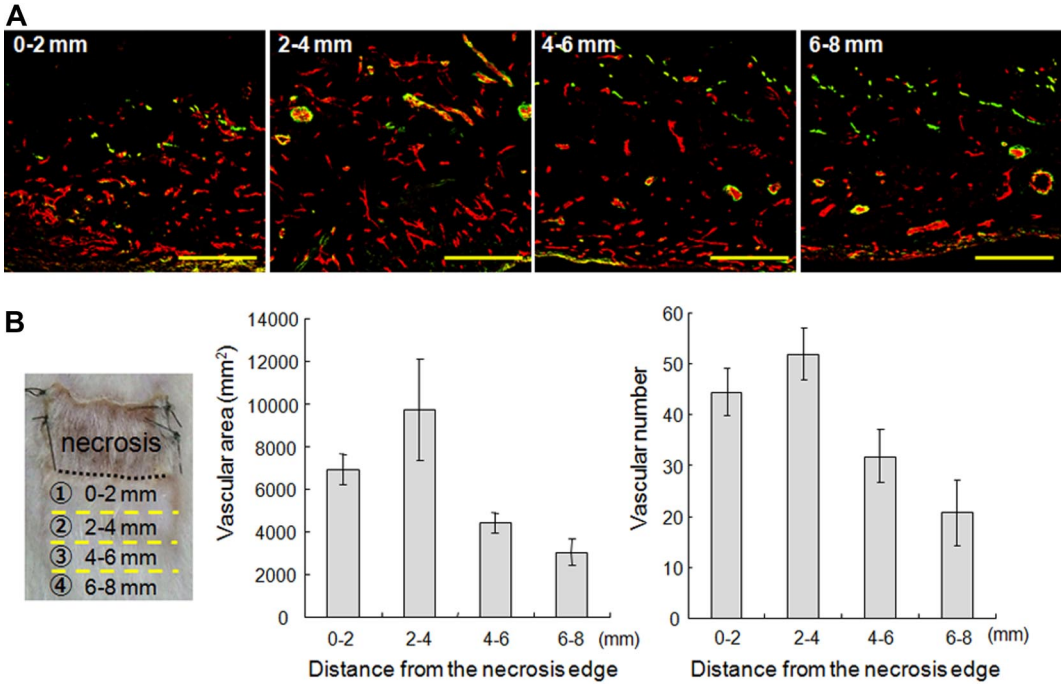

Figure 1. New vessel distribution in the skin flap. (A) The vascular distribution in the skin flap was observed in areas at every 2-mm interval from the necrotic edge. CD31 (red) is a marker for ECs, and αSMA (green) is a marker for mural cells. Scale bars are 200 μm. (B) The dashed line indicates the necrotic edge. The vascular area and vascular density per high-power field were determined from every 2-mm interval from the necrotic edge. Data are expressed as the means and SDs of each area.

endothelial basal medium (Clonetics, Walkersville, MD). THP-1, a human monocytic cell leukemia cell line was obtained from the Cell Resource Center for Biomedical Research at our institute. THP-1 cells were cultured in 10% FBS/RPMI 1640 (Nissui Pharmaceutical, Tokyo, Japan). GM7373, a chemically immortalized bovine aortic endothelial cell line, was cultured in Dulbecco modified Eagle medium (Nissui Pharmaceutical) supplemented with 10% FCS. MS1, an immortalized cell line with a SV40 large T antigen from mouse pancreatic ECs, was purchased from ATCC (Manassas, VA) and were cultured in αMEM (Invitrogen, Carlsbad, CA) supplemented with 10% FCS. All the cells were cultured at 37°C in a humidified atmosphere with 5% CO_2.

Reverse transcriptase-polymerase chain reaction analysis

Total RNA was extracted from HUVECs and THP-1 cells by the AGPC method using ISOGEN (Nippon Gene, Toyama, Japan) according to the manufacturer's instructions. Total tissue RNA was extracted from several organs of male BALB/c mice at 4 weeks or from placentas of female BALB/c mice by the AGPC method using ISOGEN-LS (Nippon Gene). First-strand cDNA was generated using a first-strand cDNA synthesis kit for reverse transcriptase–polymerase chain reaction (RT-PCR; Roche Diagnostics, Mannheim, Germany). RT-PCR was performed with a DNA thermal cycler (Takara, Tokyo, Japan). PCR conditions consisted of an initial denaturation step at 95°C for 10 minutes followed by 40 cycles consisting of 15 seconds at 95°C, 5 seconds at an indicated annealing temperature, and 15 seconds at 72°C. The primer pairs used were as follows: mouse β-actin forward, 5-ACAATGAGCTGCGTGTGGCT, and reverse, 5-TCTCCTTAATGTCACGCACGA (annealing temperature 58°C); mouse VASH1 forward, 5-AGATCCCCATACCGAGTGTG, and reverse, 5-GGGCCTCTTTGGTCATTTCC (annealing temperature 58°C); mouse VASH2 forward, 5′-ATGCCTTGAAGCTGTCATCC, and reverse, 5′-TGGCATATTTCTCCAGCTCC (annealing temperature 60°C). PCR products were analyzed by 1% or 1.5% agarose gel electrophoresis.

Quantitative real-time RT-RCR

Total RNA was extracted from the skin flap using the RNeasy Mini Kit (QIAGEN, Valencia, CA) according to the manufacturer's instructions. First-strand cDNA was generated with a first-strand cDNA synthesis kit for RT-PCR (Roche Diagnostics). Quantitative real-time RT-PCR was performed with the use of a Light Cycler System (Roche Diagnostics) according to the manufacturer's instructions. The amount of PCR product was measured as a fluorescence signal that was proportional to the amount of the specific target sequence present. PCR conditions consisted of an initial denaturation step at 95°C for 10 minutes, followed by 40 cycles consisting of 15 seconds at 95°C, 5 seconds at an indicated annealing temperature, and 15 seconds at 72°C. The primer pairs used were as follows: β-actin forward, 5-TCGTGCGTGACATCAAAGAG, and reverse, 5-TGGACAGTGAGGCCAGGATG; mouse VASH1 forward, 5-GATTCCCATACCAAGTGTGCC, and reverse, 5-ATGTGGCGGAAGTAGTTCCC (annealing temperature 62°C); mouse VASH2 forward, 5′-GGCTAAGCCTTCAATTCCCC, and reverse, 5′ CCCATTGGTGAGATAGATGCC (annealing temperature 64°C). Each mRNA level was measured as a fluorescent signal corrected according to the signal for β-actin.

Northern blot analysis

Northern blotting was performed as described.[11] Briefly, cells were starved in 0.1% FBS/αMEM. In some experiments, cells were stimulated with VEGF (Sigma-Aldrich) for 12 hours. Total RNA was then extracted by ISOGEN according to the manufacturer's instruction and was separated on a 1% agarose gel containing 2.2 M formaldehyde and transferred to a Hybond N^+ membrane. The membrane was hybridized with a ^{32}P-labeled VASH1 cDNA probe containing an open reading frame (464-1417). Autoradiography was performed on an imaging plate and analyzed with an FLA2000 (Fuji Film, Tokyo, Japan).

Intracellular localization of VASH1 and VASH2

To make a hemagglutinin (HA)–tagged construct, human VASH2 cDNA was cloned into the *Eco*R1-*Xho*1 site of internal ribosome entry site (IRES)–humanized Renilla green fluorescent protein (hrGFP) 2a vector (Stratagene, La Jolla, CA; VASH2, HA-IRES-GFP vector). To make GFP-fusion constructs, human VASH2 cDNA was cloned into CT-GFP TOPO vector (VASH2, CT-GFP vector) or NT-GFP TOPO vector (VASH2, NT-GFP vector; Invitrogen). Transfection was performed with Fugene 6 (Roche) according to the manufacturer's instructions. GFP-fusion protein was detected by the use of confocal microscopy.

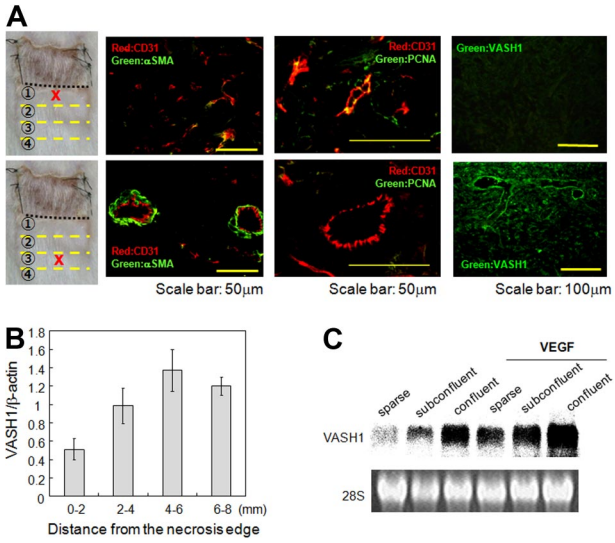

Figure 2. The spatiotemporal expression profile of VASH1. (A) Immunostaining of CD31 (red), αSMA (green), PCNA (green), and/or VASH1 (green) was performed with the indicated area of the skin flap. (B) Total RNA was isolated from each area of the skin flap. Quantitative real-time RT-PCR was performed to show mRNA levels of VASH1 in each area. Each value was standardized with β-actin. Data are expressed as mean and SDs. (C) HUVECs of sparse, subconfluent, and confluent conditions were treated with or without VEGF (1 nM) for 12 hours, and the expression of VASH1 was determined by Northern blotting.

Establishment of VASH1- or VASH2-expressing MS1 clones

To improve the activity of transcription, the CMV promoter of the pcDNA3.1/Hygro plasmid (Invitrogen) was replaced with the chicken β-actin promoter derived from pCALL2.[21] This vector, pCALL2-pcDNA3.1/Hygro, was used for the transfection in this study. Human VASH1 or VASH2 cDNA was cloned into the pCALL2-pcDNA3.1/Hygro vector at multiple cloning sites (*Xho*-I and *Not*-I). MS1 was transfected with the expression vector with the use of the Effectene transfection reagent (QIAGEN) according to the manufacturer's protocol. After the transfection, the cells were selected by hygromycin (500 μg/mL; Invitrogen).

Statistical analysis

The statistical significance of differences was evaluated by unpaired analysis of variances, and probability values were calculated with the Student *t* test. A value of *P* less than .05 was considered statistically significant.

Results

Mouse model of postnatal subcutaneous angiogenesis

To explore the roles of VASH family in the regulation of angiogenesis, we used a mouse model of postnatal subcutaneous angiogenesis. In this model, 2 parallel skin incisions were made on the back that penetrated the cutis, dermis, and underlying adipose tissue; a silicon sheet was inserted beneath the skin flap; and the incision was closed (Figure S1A, available on the *Blood* website; see the Supplemental Materials link at the top of the online article). The skin flap became hypoxic because the inserted silicon sheet blocked the blood supply from the deeper layer, and new vessels were distributed from the areas left undissected. Because of the substantial length of the skin incision, the central region became necrotic over the experimental period (Figure S1B). After 7 days, the skin flap was harvested and oriented parallel to the original incision for sectioning (Figure S2A). Pimonidazole staining showed that hypoxia was evident at the edge adjoining the necrotic tissue (Figure S2B).

We evaluated the skin flap at every 2-mm interval from the necrotic edge and determined the vessel distribution in each area (Figure 1A). In this way, the entire progress of angiogenesis could be observed from a single section. The area 0 to 4 mm from the necrotic edge contained mostly small vessels with PCNA-positive proliferating ECs (Figure 1A). This area was thus defined as the sprouting front of angiogenesis. The elevation of vascular luminal area and vascular numbers was most prevalent in the area 2 to 4 mm from the necrotic edge (Figure 1B). The area further than 4 mm from the necrotic edge contained hierarchical vasculature of small and large vessels with PCNA-negative nonproliferating ECs surrounded by αSMA-positive mural cells (Figure 1A). This area was thus defined as the termination zone of angiogenesis. Vascular luminal area and vascular numbers were decreased in this area (Figure 1B).

Spatiotemporal expression profile of VASH1 and VASH2 during angiogenesis

During the postnatal period, the expression of VASH1 and VASH2 proteins is only faintly shown in arterial ECs under the basal condition.[16] Here, we determined VASH2 mRNA in various organs

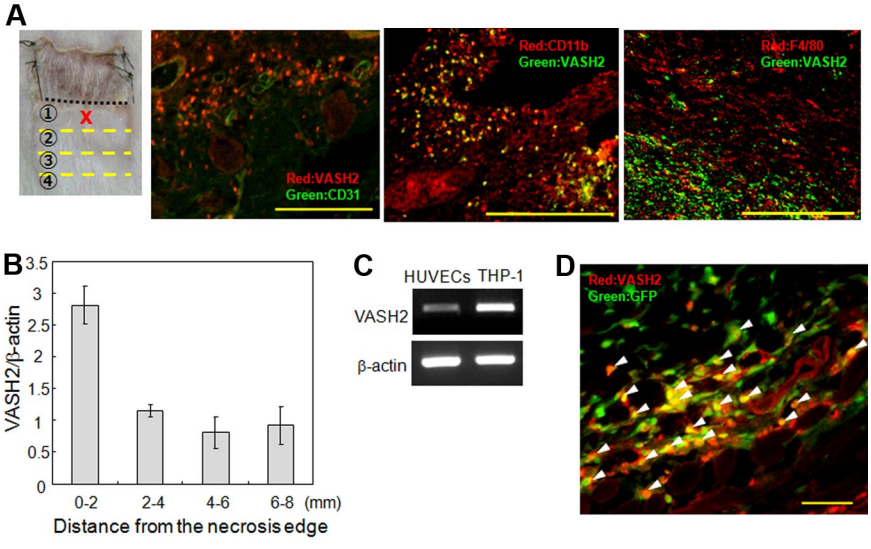

Figure 3. The spatiotemporal expression profile of VASH2. (A) Immunostaining of VASH2, CD11b, and F4/80 in the area 0 to 2 mm from the necrotic edge. Scale bars are 200 μm. (B) Total RNA was isolated from each area of the skin flap. Quantitative real-time RT-PCR was performed to show mRNA levels of VASH2 in each area. Each value was standardized with β-actin. (C) The basal level of VASH2 mRNA in HUVECs or THP-1 cells was determined by RT-PCR. (D) After confirming bone marrow reconstitution, the subcutaneous angiogenesis experiment was performed. Immunostaining of VASH2 in the area 0 to 2 mm from the necrotic edge is shown. Arrowheads indicate GFP-positive and VASH2-positive cells. Scale bar is 50 μm.

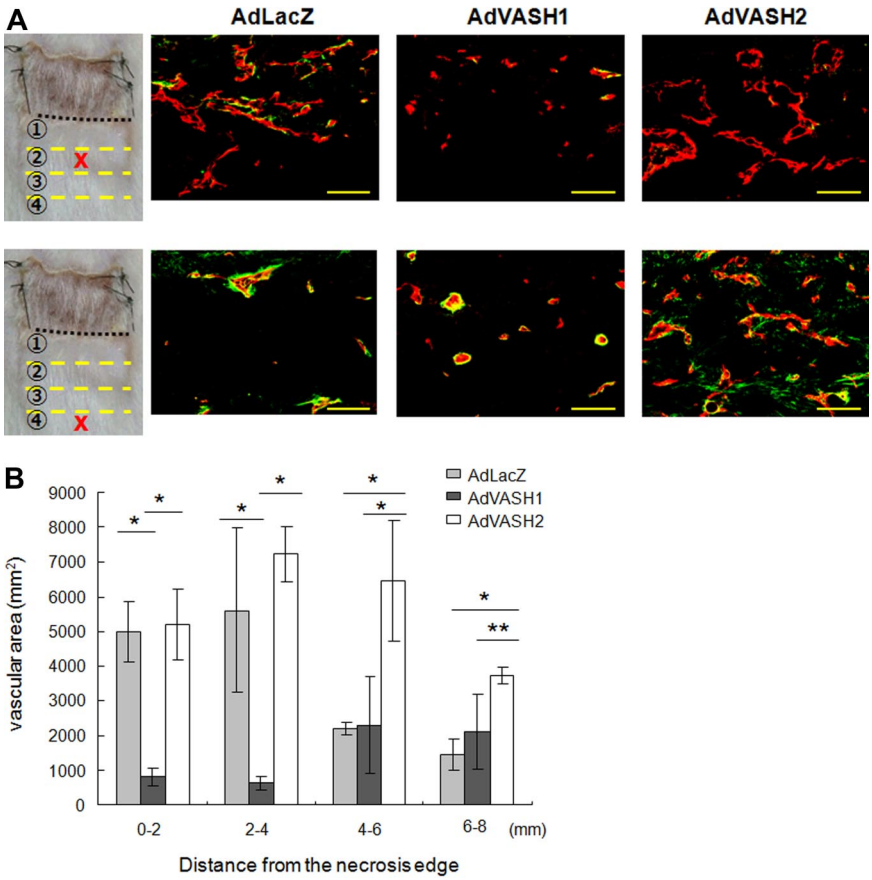

Figure 4. Effects of exogenous VASH1 or VASH2 on angiogenesis in the skin flap. AdVASH1 or AdVASH2 was injected into the tail vein to supply sufficient exogenous proteins to the site of angiogenesis. (A) Immunostaining of CD31 (red) and αSMA (green) positive cells in the indicated area of the skin flap. Scale bars are 50 μm. (B) Vascular area was determined from 5 different fields in each area. Data are expressed as the means and SDs; $^{*}P < .01$, $^{**}P < .05$.

in mice (Figure S3). This restricted expression pattern of VASH2 was comparable with that of VASH1,[11] and it further confirmed that basal expression of these 2 proteins is quite low. However, we have already reported that VASH1 is selectively present in ECs at the site of angiogenesis.[11,14,15]

Here, we determined their expression during angiogenesis more precisely. Immunostaining of VASH1 protein showed that PCNA-positive ECs in small vessels at the sprouting front were faintly stained, whereas PCNA-negative ECs surrounded by mural cells in the termination zone were intensely stained (Figure 2A). Quantitative real-time RT-PCR further confirmed that VASH1 mRNA was lowest in the area 0 to 2 mm from the necrotic edge, increased and was most prevalent in the area of 4 to 6 mm from the necrotic edge, and then declined thereafter (Figure 2B). Because VASH1 was identified as a VEFG-inducible molecule,[11] we initially thought that ECs in the sprouting front expressed VASH1 abundantly. However, it was not the case. We therefore reevaluated the expression pattern of VASH1 by using cultured HUVECs. What we found was that the expression level of VASH1 was dependent on the culture conditions. The basal expression of VASH1 in exponentially proliferating HUVECs was extremely low, increased in subconfluent to confluent cultures, although VEGF-inducibility was maintained (Figure 2C). Thus, the expression profile of VASH1 in the skin flap correlated with what we found in the culture condition.

We then determined the expression of VASH2 in this system. We noted that VASH2 protein was preferentially localized in infiltrating MNCs in the area 0 to 2 mm from the necrotic edge (Figure 3A). These MNCs were CD11b-positive but F4/80-negative (Figure 3A). Although we showed the specificity of our antibodies previously,[16] the specificity was further confirmed, because VASH1 was negative in MNCs in the sprouting front (Figure 2A), whereas VASH2 was negligible in ECs in the termination zone (Figure S4). Quantitative real-time RT-PCR further confirmed that VASH2 mRNA was highest in the area 0 to 2 mm from the necrotic edge (Figure 3B). We could also show that monocytic TPH-1 cells expressed VASH2 mRNA more abundantly than HUVECs (Figure 3C).

It has been well accepted that bone marrow–derived cells contribute to angiogenesis.[22] We therefore hypothesized that these MNCs were derived from bone marrow. To prove this, we lethally irradiated wild-type mice and transplanted them with bone marrow cells from mice ubiquitously expressing green fluorescent protein (GFP-mice). After confirming bone marrow reconstitution, we performed the subcutaneous angiogenesis analysis. We observed that most of the VASH2-positive MNCs were positive for GFP (Figure 3D arrowheads). We could hardly detect GFP-positive cells integrated in the wall of neo-vessels.

These results indicate that VASH1 is expressed by ECs in the termination zone, whereas VASH2 is mainly expressed by bone marrow–derived MNCs infiltrating the sprouting front.

Effects of exogenous VASH1 or VASH2 on angiogenesis

To evaluate the effect of exogenous VASH1 or VASH2, we injected AdVASH1 or AdVASH2 into the tail vein of mice to cause expression of these genes in the liver. We confirmed the expression of VASH1 or VASH2 in the liver (data not shown). As described previously, this procedure supplied sufficient proteins to regulate angiogenesis in the remote site.[15] Adenovirus-mediated transfer of the *VASH1* gene inhibited angiogenesis at the sprouting front where endogenous VASH1 was scarce, but it did not influence vascularity in the termination zone where endogenous VASH1 was enriched (Figure 4A,B). Adenoviral-mediated transfer of the *VASH2* gene

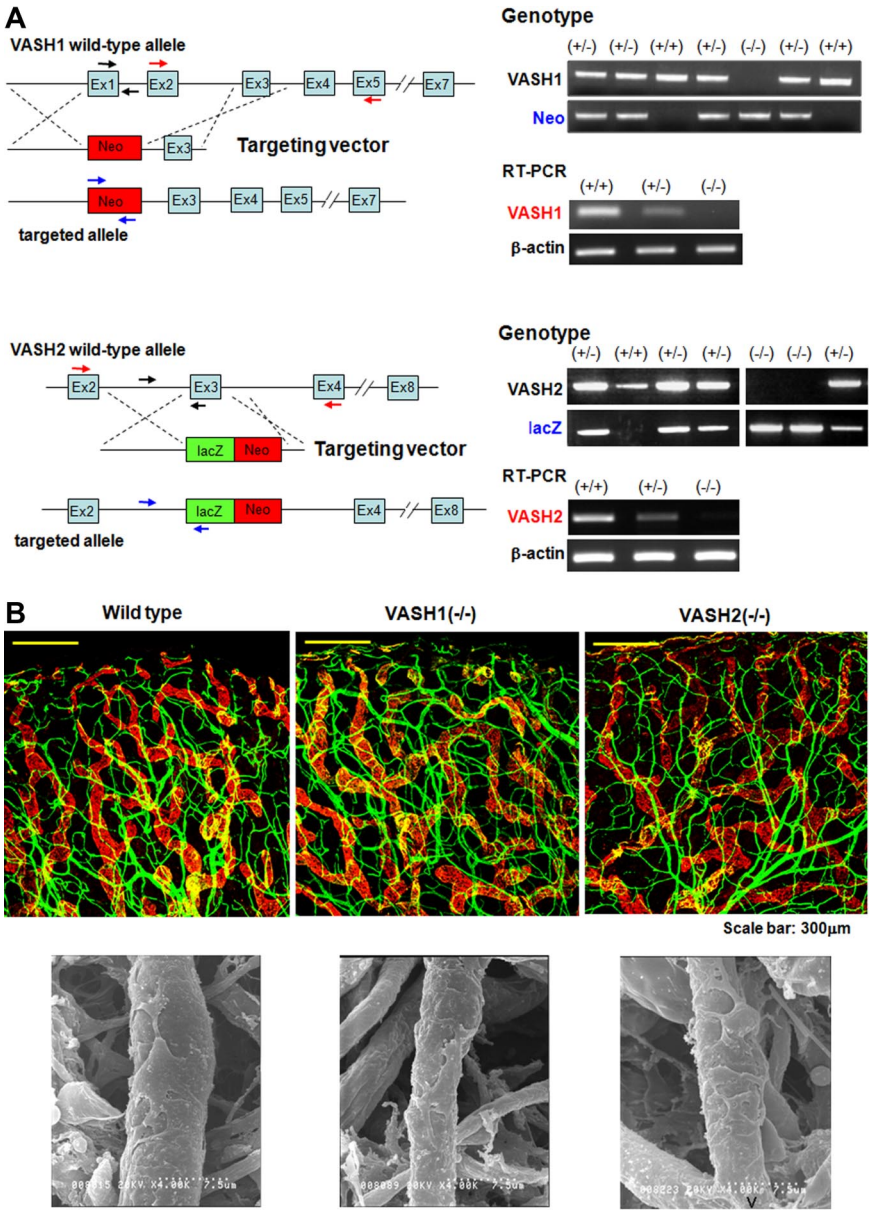

Figure 5. Generation of *VASH1* and *VASH2* knockout mice and their steady state subcutaneous vascular architecture. (A) *VASH1* and *VASH2* knockout mice were generated as described in "Generation of VASH1 and VASH2 knockout mice." Genotyping and the analysis of each transcript by RT-PCR are shown. (B) Ear skin was used to show the steady state vascular architecture of ear skin. Top panels show immunostaining of CD31 (green) and LYVE-1 (red). Bottom panels show SEM of capillary vessels.

did not cause any changes in the sprouting front, but it sustained the increased vascularity in the termination zone (Figure 4A,B). These opposing effects of VASH1 and VASH2 were further confirmed in vitro by the stable transfection of the *VASH1* or *VASH2* gene into cultured ECs (Figure S5). Both VASH1 and VASH2 lack classical signal sequences.[11,16] We have previously shown that VASH1 is an endoplasmic reticulum–independent secretory protein. To compare the intracellular localization of VAS1 and VASH2 proteins, we constructed the GFP-fused human *VASH2* expression vectors and transfected them into GM7373 cells. We simultaneously transfected human *VASH1* gene with the use of AdVASH1. As shown in Figure S6, the intracellular localization of VASH1 and VASH2 was comparable. In consequence, exogenous VASH1 inhibits angiogenesis at the sprouting front, whereas exogenous VASH2 prolongs angiogenesis in the termination zone.

Function of endogenous VASH1 or VASH2 on angiogenesis

To further clarify the function of endogenous VASH1 and VASH2, we generated *VASH1* or *VASH2* knockout mice by conventional homologous recombination (Figure 5A). We examined the steady state vascular architecture of ear subcutis of survived mice. We could not find any significant changes of vascular architecture in either *VASH1* knockout or *VASH2* knockout mice (Figure 5B).

We then subjected the *VASH1* knockout and *VASH2* knockout mice to the model of subcutaneous angiogenesis. The degree of vascular area at the sprouting front was almost identical between wild-type, *VASH1*$^{+/-}$, and *VASH1*$^{-/-}$ mice (Figure 6B). The vascular area significantly decreased in the termination zone in the wild-type mice where endogenous VASH1 was enriched, but that was maintained in higher degree in *VASH1* knockout mice (Figure 6A). Quantitative analysis showed that this change was gene-dosage sensitive (Figure 6B). Lectin staining indicated that new vessels of *VASH1*$^{-/-}$ mice were patent and maintained blood flow (Figure 6C). Supplementation of the deficient proteins by adenoviral-mediated gene transfer normalized the abnormal angiogenesis patterns in *VASH1* knockout (Figure 6D).

In contrast, the vascular density was lower in entire areas in the *VASH2* knockout mice (Figure 7B). This change was gene-dosage

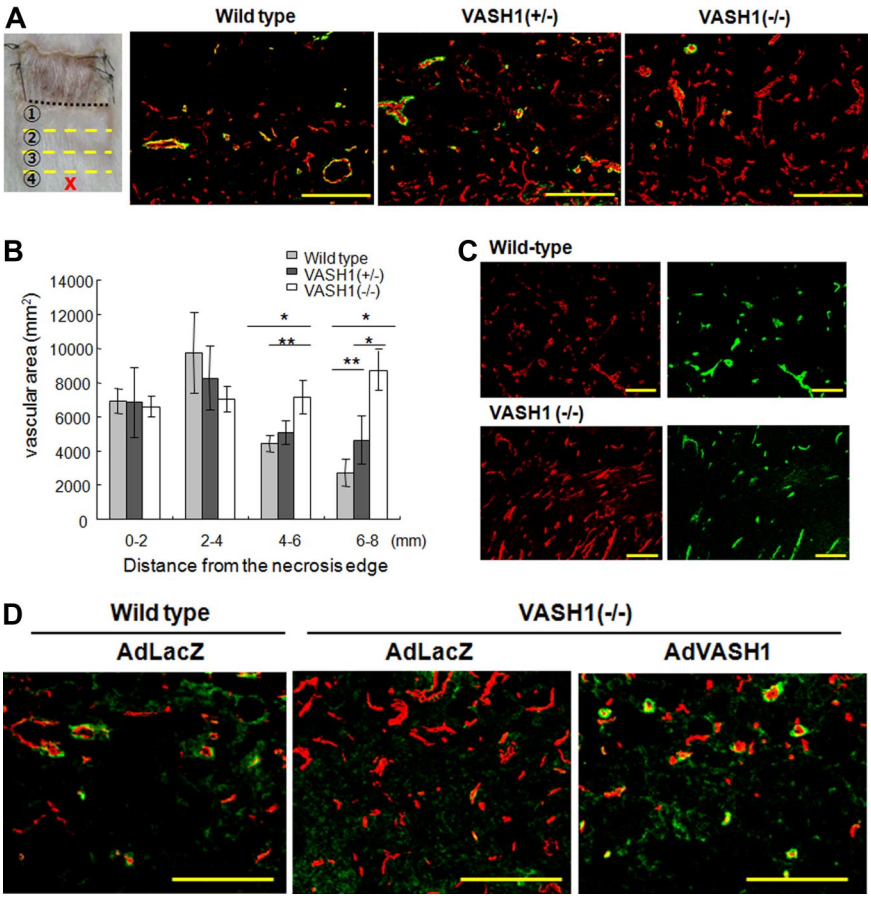

Figure 6. Vascular distribution in the skin flap of *VASH1* knockout mice. *VASH1* knockout mice were applied to the model of subcutaneous angiogenesis. (A) Immunostaining of CD31 (red) and αSMA (green) in the area 6 to 8 mm from the necrotic edge is shown. Scale bars are 200 μm. (B) The vascular area was determined from 5 different fields in each area. Data are expressed as the means and SDs; $^{*}P < .01$, $^{**}P < .05$. (C) Lectin staining (green) shows the perfusion of new vessels in the area 6 to 8 mm from the necrotic edge. The same section was immunostained for CD31 (red). Scale bars are 200 μm. (D) Adenoviral-mediated gene transfer was performed to supplement the deficient protein in *VASH1* knockout mice. AdLacZ was use as the control. Immunostaining of CD31 (red) and αSMA (green) in the indicated area of the skin flap is shown. Scale bars are 200 μm.

sensitive at the sprouting front where endogenous VASH2 should be enriched (Figure 7A,B). Importantly, the extent of MNC infiltration in the sprouting front was not altered in *VASH2*$^{-/-}$ mice (Figure 7C). Again, supplementation of the deficient proteins by adenoviral-mediated gene transfer normalized the abnormal angiogenesis patterns in *VASH2* knockout mice (Figure 7D).

Discussion

We characterized the roles of the 2 members of the vasohibin family in the regulation of angiogenesis with the use of a mouse model of subcutaneous angiogenesis. The spatiotemporal expression pattern and substantial effects of these 2 molecules indicate that VASH1 and VASH2 control the promotion and termination of angiogenesis in a complementary manner.

The expression of endogenous VASH1 was augmented in nonproliferating ECs in the termination zone of postnatal angiogenesis. This VASH1 in the termination zone should be involved in halting angiogenesis, because angiogenesis persisted in the termination zone in *VASH1* knockout mice in a gene-dosage manner. This result also implies that endogenous VASH1 is not a principal regulator limiting the sprouting. However, when applied exogenously, VASH1 can inhibit angiogenesis at the sprouting front where endogenous VASH1 is scarce. In addition, exogenous VASH1 exhibits little effect, if any, in the termination zone where endogenous VASH1 is present. Accordingly, the present results show the distinctive acting points of endogenous and exogenous VASH1 and further support the legitimacy of using exogenous VASH1 as an antiangiogenic treatment.

Endogenous VASH2, in contrast, was expressed mainly by infiltrating bone marrow–derived MNCs at the sprouting front in our model. The present result contrasts with our previous observation about VASH2 expression in ECs of developing embryos without obvious MNC infiltration.[16] About the expression of VASH2 in MNCs, monocytic THP-1 cells were found to express VASH2 more abundantly than ECs in culture. Hence, MNCs can be the main source of VASH2 when they infiltrate.

Bone marrow–derived cells, including endothelial progenitor cells (EPCs), contribute to postnatal angiogenesis.[22] However, we could hardly detect the integration of bone marrow–derived cells in the neo-vessels in our model, indicating that EPCs might not play a major role in our model. What we observed was that most of the bone marrow–derived cells infiltrated in the sprouting front were MNCs. It is described that bone marrow–derived MNCs stimulate angiogenesis by producing angiogenic factors, including VEGF and several matrix metalloproteinases.[23,24] Along these lines, we propose that VASH2 produced by bone marrow–derived MNCs takes part in the promotion of postnatal angiogenesis, because angiogenesis at the sprouting front is significantly impaired in *VASH2* knockout mice even in the presence of MNC infiltration. Appropriately, exogenous VASH2 inhibited the termination of angiogenesis in the termination zone where endogenous VASH2 staining was faint.

We previously reported that, when applied exogenously, VASH-2 exhibited the antiangiogenic activity in the mouse cornea.[16] However, to our surprise, the present study rather indicated the proangiogenic activity of VASH2. Amino acid sequence of VASH2 is 52.5% homologous to that of VASH1 in humans, and 51.9% homologous in mice.[16] We therefore hypothesize the role of

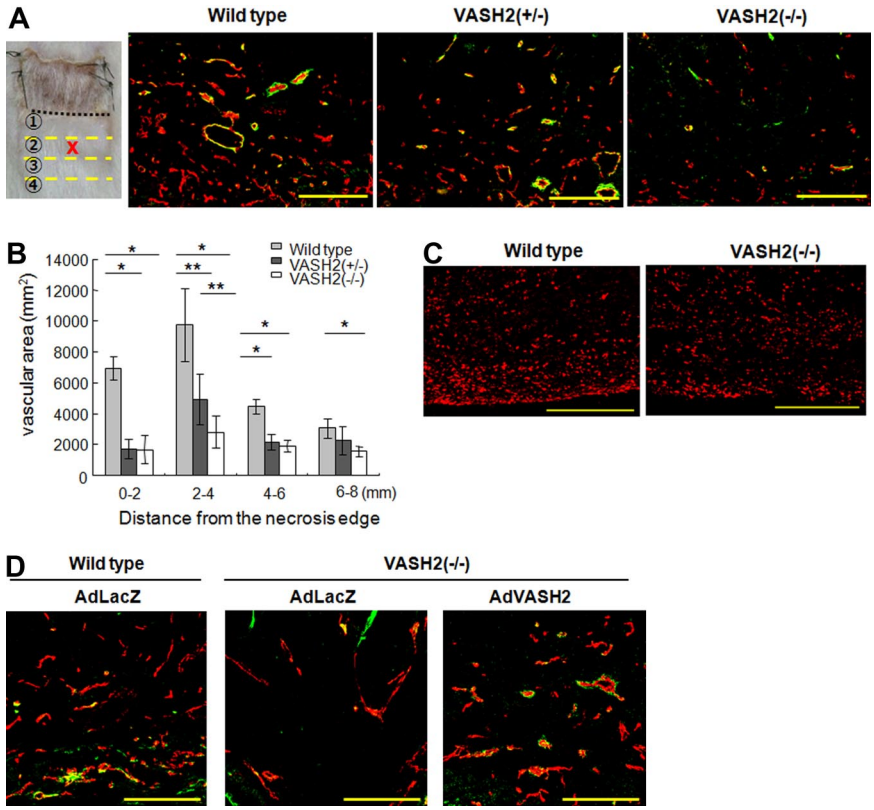

Figure 7. Vascular distribution in the skin flap of *VASH2* knockout mice. *VASH2* knockout mice were applied to the model of subcutaneous angiogenesis. (A) Immunostaining of CD31 (red) and αSMA (green) in the area 2 to 4 mm from the necrotic edge is shown. Scale bars are 200 μm. (B) The vascular area was determined from 5 different fields in each area. Data are expressed as the means and SDs; $*P < .01$, $**P < .05$. (C) Immunostaining of CD11b (red) in the area 0 to 2 mm from the necrotic edge is shown in wild-type and *VASH2*$^{-/-}$ mice. Scale bars are 200 μm. (D) Adenoviral-mediated gene transfer was performed to supplement the deficient protein in *VASH2* knockout mice. AdLacZ was use as the control. Immunostaining of CD31 (red) and αSMA (green) in the indicated area of the skin flap is shown. Scale bars are 200 μm.

VASH2 as follows. On the analogy to angiopoietin-1 and angiopoietin-2, VASH1 and VASH2 may share the same receptor. VASH2 is a weak agonist and antagonizes VASH1 in a certain condition, although the receptor for the VASH family is not yet identified. We are currently testing this hypothesis.

There are several endogenous angiogenesis inhibitors in the body, but it is still not clear why the body needs so many angiogenesis inhibitors. Systematic analysis to show how these endogenous angiogenesis inhibitors orchestrate the control of angiogenesis is lacking. Delta-like 4 (Dll4) is the ligand of Notch1, which determines the arterial specification of ECs.[25,26] However, recent evidence indicates that ECs at the sprouting tip express Dll4 and that this Dll4 negatively regulates the formation of appropriate numbers of sprouting tips.[27-31] Therefore, Dll4 and VASH1 are 2 inhibitors that are expressed in ECs, but the apparent difference between VASH1 and Dll4 is their temporal expression patterns. Dll4 is selectively expressed in tip cells, whereas VASH1 is expressed in ECs in the termination zone. Hence, VASH1 and Dll4 are expressed in different phases of angiogenesis and should negatively tune this phenomenon distinctively. It is described that inactivation of Dll4 increases sprouting microvessels without proper blood perfusion.[32,33] Importantly, increased numbers of microvessels in the termination zone of *VASH1*$^{-/-}$ mice were patent and maintained blood perfusion. This difference in blood perfusion further proposes the distinctive roles of VASH1 and Dll4 in the regulation of angiogenesis.

In summary, the vasohibin family members, VASH1 and VASH2, participate in the regulation of angiogenesis in a previously unrecognized manner. VASH1 is expressed in ECs in the termination zone to halt angiogenesis, whereas VASH2 is expressed mainly in infiltrating MNCs at the sprouting front to promote angiogenesis. Discovery of these molecules should provide novel approaches to both antiangiogenic and proangiogenic treatments. Further study is currently under way to clarify the underlying mechanism how VASH1 and VASH2 regulate angiogenesis in an opposed but complementary manner.

Acknowledgments

This work was supported by a Grant-in-Aid for Scientific Research on Priority Areas of the Japanese Ministry of Education, Science, Sports, and Culture from the Ministry of Education, Science, Sports, and Culture of Japan (contract grants 16022205 and 17014006), and by the 21st Century COE Program Special Research Grant "The Center for Innovative Therapeutic Development Towards the Conquest of Signal Transduction Diseases" from the Ministry of Education, Science, Sports, and Culture of Japan.

Authorship

Contribution: H.K. performed research and wrote the paper; H.M. and Y.S. prepared the knockout mice; M.K. performed transfection to MS1 cells; K.W. performed analysis of the intracellular localization; H.S. and H.O. prepared antibodies; T.F. performed electron microscopy; T.S. designed the research; and Y.S. designed the research and wrote the paper.

Conflict-of-interest disclosure: The authors declare no competing financial interests.

Correspondence: Yasufumi Sato, Department of Vascular Biology, Institute of Development, Aging and Cancer, Tohoku University, 4-1 Seiryo-machi, Aoba-ku, Sendai 980-8575, Japan; e-mail: y-sato@idac.tohoku.ac.jp.

References

1. Adams RH, Alitalo K. Molecular regulation of angiogenesis and lymphangiogenesis. Nat Rev Mol Cell Biol. 2007;8:464-478.
2. Sato Y. Update on endogenous inhibitors of angiogenesis. Endothelium. 2006;13:147-155.
3. Dawson DW, Volpert OV, Gillis P, Crawford SE, et al. Pigment epithelium-derived factor: a potent inhibitor of angiogenesis. Science. 1999;285:245-248.
4. Renno RZ, Youssri AI, Michaud N, Gragoudas ES, Miller JW. Expression of pigment epithelium-derived factor in experimental choroidal neovascularization. Invest Ophthalmol Vis Sci. 2002;43:1574-1580.
5. Hiraki Y, Inoue H, Iyama K, et al. Identification of chondromodulin I as a novel endothelial cell growth inhibitor. Purification and its localization in the avascular zone of epiphyseal cartilage. J Biol Chem. 1997;272:32419-32426.
6. Yoshioka M, Yuasa S, Matsumura K, et al. Chondromodulin-I maintains cardiac valvular function by preventing angiogenesis. Nat Med. 2006;12:1151-1159.
7. Zhang M, Volpert O, Shi YH, Bouck N. Maspin is an angiogenesis inhibitor. Nat Med. 2000;6:196-199.
8. Maass N, Nagasaki K, Ziebart M, Mundhenke C, Jonat W. Expression and regulation of tumor suppressor gene maspin in breast cancer. Clin. Breast Cancer. 2002;3:281-287.
9. Kopp HG, Hooper AT, Broekman MJ, et al. Thrombospondins deployed by thrombopoietic cells determine angiogenic switch and extent of revascularization. J Clin Invest. 2006;116:3277-3291.
10. Kalluri R. Basement membranes: structure, assembly and role in tumour angiogenesis. Nat Rev Cancer. 2003;3:422-433.
11. Watanabe K, Hasegawa Y, Yamashita H, et al. Vasohibin as an endothelium-derived negative feedback regulator of angiogenesis. J Clin Invest. 2004;114:884-886.
12. Shimizu K, Watanabe K, Yamashita H, et al. Gene regulation of a novel angiogenesis inhibitor, vasohibin, in endothelial cells. Biochem Biophys Res Commun. 2005;327:700-7006.
13. Sonoda H, Ohta H, Watanabe K, Yamashita H, Kimura H, Sato Y. Multiple processing forms and their biological activities of a novel angiogenesis inhibitor vasohibin. Biochem Biophys Res Commun. 2006;342:640-646.
14. Shen JK, Yang XR, Sato Y, Campochiaro PA. Vasohibin is up-regulated by VEGF in the retina and suppresses VEGF receptor 2 and retinal neovascularization. FASEB J. 2006;20:723-725.
15. Yamashita H, Abe M, Watanabe K, et al. Vasohibin prevents arterial neointimal formation through angiogenesis inhibition. Biochem Biophys Res Commun. 2006;345:919-925.
16. Shibuya T, Watanabe K, Yamashita H, et al. Isolation of vasohibin-2 as a sole homologue of VEGF-inducible endothelium-derived angiogenesis inhibitor vasohibin: a comparative study on their expressions. Arterioscler Thromb Vasc Biol. 2006;26:1051-1057.
17. Sato Y, Sonoda H. The vasohibin family: a negative regulatory system of angiogenesis genetically programmed in endothelial cells. Arterioscler Thromb Vasc Biol. 2007;27:37-41.
18. Tepper OM, Capla JM, Galiano RD, et al. Adult vasculogenesis occurs through in situ recruitment, proliferation, and tubulization of circulating bone marrow-derived cells. Blood. 2005;105:1068-1077.
19. Oike Y, Akao M, Yasunaga K, et al. Angiopoietin-related growth factor antagonizes obesity and insulin resistance. Nat Med. 2005;11:400-408.
20. Yamazaki D, Suetsugu S, Miki H, et al. WAVE2 is required for directed cell migration and cardiovascular development. Nature. 2003;424:452-456.
21. Namba K, Abe M, Saito S, et al. Indispensable role of the transcription factor PEBP2/CBF in angiogenic activity of a murine endothelial cell MSS31. Oncogene. 2000;19:106-114.
22. Rabbany SY, Heissig B, Hattori K, Rafii S. Molecular pathways regulating mobilization of marrow-derived stem cells for tissue revascularization. Trends Mol Med. 2003;9:109-117.
23. Barbera-Guillem E, Nyhus JK, Wolford CC, Friece CR, Sampsel JW. Vascular endothelial growth factor secretion by tumor-infiltrating macrophages essentially supports tumor angiogenesis, and IgG immune complexes potentiate the process. Cancer Res. 2002;62:7042-7049.
24. Cho CH, Koh YJ, Han J, et al. Angiogenic role of LYVE-1-positive macrophages in adipose tissue. Circ Res. 2007;100:e47-57.
25. Shutter JR, Scully S, Fan W, et al. Dll4, a novel Notch ligand expressed in arterial endothelium. Genes Dev. 2000;14:1313-1318.
26. Duarte A, Hirashima M, Benedito R, et al. Dosage-sensitive requirement for mouse Dll4 in artery development. Genes Dev. 2004;18:2474-2478.
27. Williams CK, Li JL, Murga M, Harris AL, Tosato G. Up-regulation of the Notch ligand Delta-like 4 inhibits VEGF-induced endothelial cell function. Blood. 2006;107:931-939.
28. Hellstrom M, Phng LK, Hofmann JJ, et al. Dll4 signalling through Notch1 regulates formation of tip cells during angiogenesis. Nature. 2007;445:776-780.
29. Siekmann AF, Lawson ND. Notch signalling limits angiogenic cell behaviour in developing zebrafish arteries. Nature. 2007;445:781-784.
30. Leslie JD, Ariza-McNaughton L, Bermange AL, McAdow R, Johnson SL, Lewis J. Endothelial signaling by the Notch ligand Delta-like 4 restricts angiogenesis. Development. 2007;134:839-844.
31. Lobov IB, Renard RA, Papadopoulos NJ, et al. Delta-like ligand 4 (Dll4) is induced by VEGF as a negative regulator of angiogenic sprouting. Proc Natl Acad Sci U S A. 2007;104:3219-3224.
32. Noguera-Troise I, Daly C, Papadopoulos NJ, et al. Blockade of Dll4 inhibits tumour growth by promoting nonproductive angiogenesis. Nature. 2006;444:1032-1037.
33. Ridgway J, Zhang G, Wu Y, et al. Inhibition of Dll4 signalling inhibits tumour growth by deregulating angiogenesis. Nature. 2006;444:1083-1087.